Estuaries and Coasts
DOI 10.1007/s12237-016-0195-9

Salinity Variability and Water Exchange in Interconnected Estuaries

Yuntao Wang[1,2] · **Renato M. Castelao**[1] · **Daniela Di Iorio**[1]

Received: 7 July 2016 / Revised: 5 November 2016 / Accepted: 10 November 2016
© Coastal and Estuarine Research Federation 2016

Abstract A high-resolution coastal ocean model is used to investigate salinity variability and water exchange in a complex coastal system off the southern U.S. characterized by three adjacent sounds that are interconnected by a network of channels, creeks, and intertidal areas. Model results are generally highly correlated with observations from the Georgia Coastal Ecosystem Long Term Ecological Research (GCE-LTER) program, revealing a high degree of salinity variability at the Altamaha River and Doboy Sound, decreasing sharply toward Sapelo Sound. A Lagrangian particle tracking method is used to investigate local residence time and connectivity in the system. Local residence time is highly variable, increasing with distance from the Altamaha River and decreasing with river flow, revealing that discharge plays a dominant role on transport processes and estuary-shelf exchange. The Altamaha River and Doboy Sound are connected to each other in all seasons, with exchange occurring both via coastal and estuarine pathways. While particles released at the Altamaha and Doboy rarely reach Sapelo Sound, particles released at Sapelo Sound and the creeks surrounding its main channel can reach the entire estuarine system.

Communicated by Carl T. Friedrichs

✉ Renato M. Castelao
castelao@uga.edu

[1] Department of Marine Sciences, University of Georgia, Athens, GA 30602, USA

[2] NOAA Fisheries Office of Science and Technology, Silver Spring, MD 20910, USA

Keywords Residence time · Connectivity · FVCOM · Exchange

Introduction

The Georgia coast is a complex estuarine system, with sounds connected by a network of channels, creeks, and intertidal areas (Di Iorio and Castelao 2013). Located at the central coast of Georgia around Sapelo Island, the Altamaha River and Doboy and Sapelo Sounds (Fig. 1) are connected to each other. The dominant source of freshwater to the system is the Altamaha River, which is one of the largest rivers in the southeastern U.S. (Sheldon and Burd 2014). Maximum river runoff occurs during spring (Menzel 1993), although a secondary peak in river discharge can also be observed in some years during fall (Blanton and Atkinson 1983). The frequency of occurrence of anomalously low-discharge conditions in the Altamaha River seems to have increased over the last decades (Medeiros et al. 2015). This long-term decrease in freshwater delivery to the estuary has been at least partially linked to freshwater withdrawal within the watershed (Fanning 2003).

River discharge is the dominant factor controlling salinity variability in the Altamaha-Doboy-Sapelo estuarine complex (Di Iorio and Castelao 2013). In addition to density-driven circulation, tides and wind forcing are also well recognized to be important drivers of horizontal exchange between estuaries and the coastal ocean (Geyer and Signell 1992). The South Atlantic Bight off the coast of Georgia is characterized by large semidiurnal tides, ranging from 1.8 m during neap to 2.4 m during spring tides (Di Iorio and Castelao 2013). Semidiurnal tides can account for roughly 80% of the kinetic energy over the inner- and mid-shelf (Pietrafesa et al. 1985). The tidal band can also account for 80–90% of the cross-shelf and 20–40% of the alongshelf current variance (Tebeau and

Published online: 21 November 2016

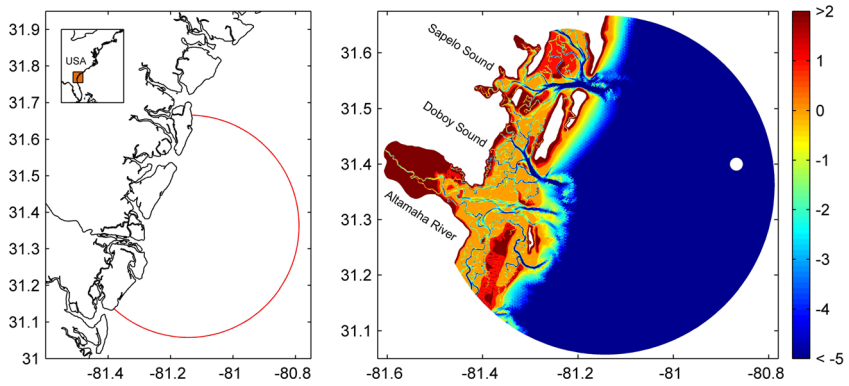

Fig. 1 Model domain with bottom topography (colors, in meters). *Red line* on left panel shows offshore model boundary. *White circle* offshore on right panel indicates the location of NOAA National Data Buoy Center buoy 41008 where wind measurements were obtained

Lee 1979; Lee and Brooks 1979). As such, tides can contribute substantially for estuary-shelf exchange in the South Atlantic Bight.

Wind forcing in the region is characterized by strong seasonal variability. Winds are predominantly northeastward (i.e., upwelling favorable) during summer and southwestward (i.e., downwelling favorable) during fall (Fig. 2; Weber and Blanton 1980; Blanton et al. 2003). Winds are less persistent during spring and winter, although an offshore component is clearly recognizable in winter (Menzel 1993). Southwestward winds are generally associated with relative increases in salinity at the mouth of the Altamaha River, and with decreases in salinity at Doboy and Sapelo Sounds (Di Iorio and Castelao 2013). Alongshore currents generally follow the seasonal wind regime, being poleward during summer and equatorward during fall (Bumpus 1973; Weber and Blanton 1980; Atkinson et al. 1983);

Estuarine circulation and estuary-shelf exchange have a major impact on the ecology, chemistry, water quality, and sedimentary processes in estuarine and coastal environments (Geyer and Signell 1992). In particular, the residence time, the average time a water particle spends within the estuary, or in some portion thereof (Geyer and Signell 1992), is crucially important for a number of ecological processes (Church 1986; Alpine and Cloern 1992; Rasmussen and Josefson 2002; Duarte and Vieira 2009), including water contamination and nutrient levels, distributions of organics, and their spatio-temporal variations in bays and estuaries (Aikman and Lanerolle 2004). Residence time is a local measure (i.e., it is spatially variable within the domain; Monsen et al. 2002), and as such it is referred to as local residence time here. We consider the time for a particle or water parcel to leave the estuary for the first time, in contrast to accounting for subsequent reentries due to the tidal nature of estuaries (De Brauwere et al. 2011). River discharge (Alber and Sheldon 1999b; Lemagie and Lerczak 2015), winds (Geyer 1997), and tidal forcing (Lemagie and Lerczak 2015) can influence the local residence time. Previous studies have also shown that river discharge is an important factor determining flushing time (the time required for the freshwater inflow to equal the amount of freshwater originally present in the estuary; Sheldon and Alber 2002) in the Altamaha River. Short flushing times are generally associated with large river discharge while comparatively longer flushing times are usually observed during periods of low flow, although the dependence is not always linear (Alber and Sheldon 1999a). Using box models, Sheldon and Alber (2002) showed that the flushing time in the Altamaha River generally ranges between 1 and 6 days depending on river flow. However, these studies assumed a simplified geometry, not fully considering possible connections between the Altamaha River and Doboy and Sapelo Sounds farther north. In fact, most previous estuarine studies have focused on a single estuary and its connection with the coastal ocean. The comparatively few existing studies addressing multi-inlet estuaries (e.g., Traynum and Styles 2008; Zhao et al. 2010) have shown that the flow in that case can be driven by mutual forcing between the adjacent inlets. Using a simple idealized numerical model setup, Di Iorio and Castelao (2013) noticed that the network of creeks and channels connecting the Altamaha River and Doboy sound could also play a large role in water exchange between the subdomains since the channels offer an alternative pathway for exchange.

In this paper, we use a high-resolution coastal ocean model to investigate salinity variability and water exchange in interconnected estuaries off the Georgia coast characterized by complex geometry. The model implementation is described in "Methods" section, followed by model evaluation and identification of salinity variability in "Model Evaluation and Salinity Variability in the System" section. We quantify local residence time in the system and how it varies seasonally in "Local residence time" section. Transport pathways in the system (i.e., the pathways by which particles move between different sectors of the estuarine system) are identified in "Connectivity and Transport Pathways" section, providing insight of connectivity among the different estuaries. Connectivity is defined for each location along the estuary as all the different sectors of the estuarine system visited by a particle released at that location. If a particle released at a given location at the Altamaha River is transported into

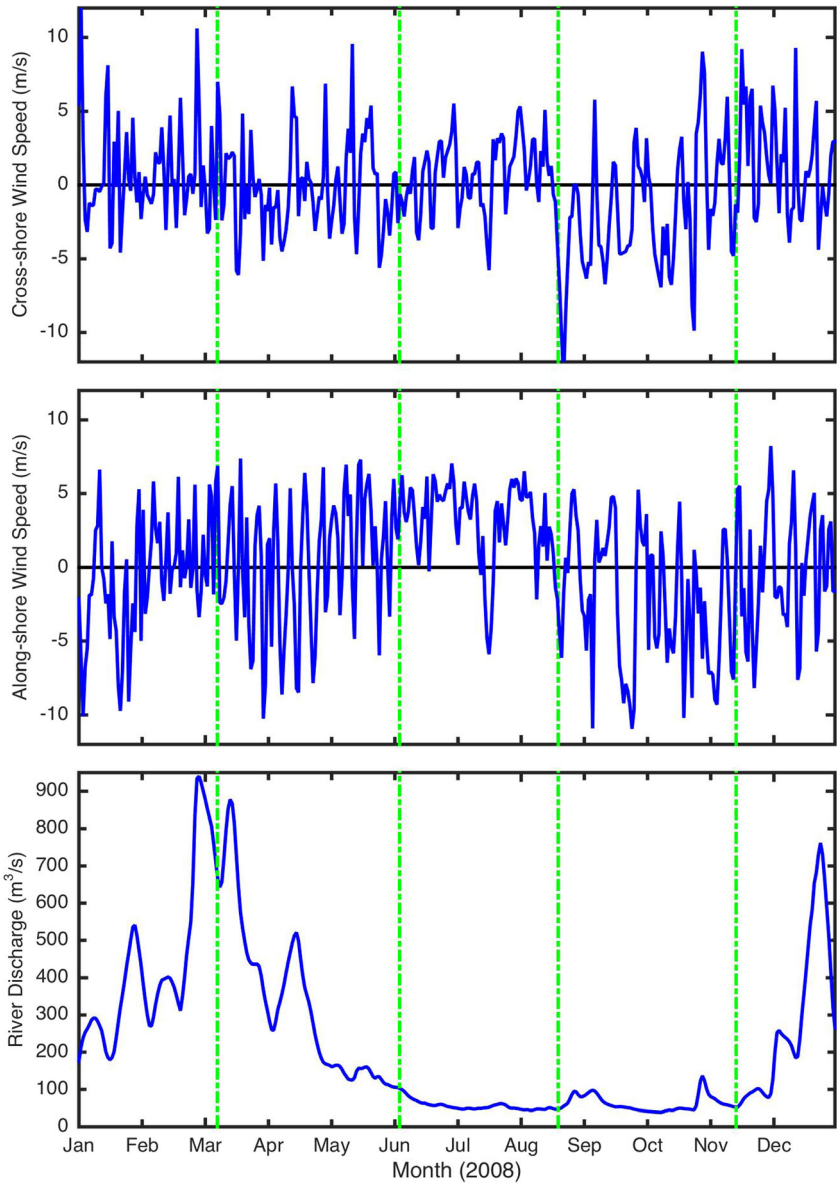

Fig. 2 Time series of cross-shelf (*top*) and alongshelf (*middle*) wind speed and of river discharge (*bottom*) during 2008. *Vertical green lines* indicate the timing of Lagrangian particle releases in the model. Positive alongshelf winds are upwelling favorable, while negative alongshelf winds are downwelling favorable

Doboy Sound but not into Sapelo Sound, for example, then that location is considered to be connected to Doboy Sound and not connected to Sapelo Sound. Results are summarized and conclusions are presented in "Conclusions" section.

Methods

The numerical modeling effort was based on the Finite Volume Community Ocean Model (FVCOM; Chen et al. 2006a, b, 2007, 2008). We chose to use FVCOM because it allows the use of unstructured grids and because of its wetting and drying capability, which are important features to model circulation in estuaries characterized by complex geometry and bathymetry. FVCOM has been successfully used to model the Satilla River Estuary off the Georgia coast (Chen et al. 2008), which presents complex geometry similar to the study region. FVCOM has also been recently used in a wide variety of estuarine studies (Ralston et al. 2010; Zhao et al. 2010; Lemagie and Lerczak 2015).

The spatial domain covers the estuarine complex, from the Altamaha River in the south to Sapelo Sound in the north (Fig. 1). Bottom topography over the entire domain was obtained from the National Oceanic and Atmospheric Administration (NOAA) National Geophysical Data Center, Coastal Relief Model. The horizontal resolution of the model is 30–70 m in tidal creeks and over salt marshes and 100–200 m in the main water channels. The grid scale increases slowly over the shelf to about 1.2 km near the open boundary. The horizontal resolution used here is comparable to the resolution used in other estuarine studies using FVCOM (Chen et al. 2008; Ralston et al. 2010; Zhao et al. 2010). The total

number of triangular elements and nodes are 351,731 and 177,796, respectively. In the vertical dimension, six layers are specified in the generalized terrain-followed σ-coordinate system, similarly to Zhao et al. (2010). The Coriolis parameter is constant, matching the value near the center of the domain ($f = 7.6114 \times 10^{-5}$ s^{-1}). The model incorporates the Mellor and Yamada (1982) 2.5-level turbulence closure scheme.

At the open boundaries, the model was forced by eight tidal constituents (M2, S2, N2, K2, K1, P1, O1, and Q1) that were extracted from the Oregon State University tidal model (Egbert and Erofeeva 2002). As in Lemagie and Lerczak (2015), time variations in offshore stratification along the boundaries were excluded. Winds were measured at the NOAA National Data Buoy Center (NDBC) buoy 41008 located at 31.40°N, 80.87°W (Fig. 1). Because of the lack of spatially resolving meteorological observations and considering the relative small extent of the model domain, winds were considered spatially uniform in the model simulations. Freshwater discharge input at the head of the Altamaha River was obtained from the United States Geological Survey gauge at Doctortown. Measurements are available at hourly intervals since 1931. The ungauged area within the Altamaha River watershed constitutes less than 3% of the river discharge (Alber and Sheldon 1999a). Moore (1996) has suggested that freshwater input from groundwater discharge can be important in coastal regions along the South Atlantic Bight, with relatively large seasonal variability (Moore 2010). However, no quantitative assessment of the magnitude of the input is available for the study region. Groundwater input was not considered in the model implementation. Possibly as a result of neglecting that input, preliminary tests indicated that modeled salinity at Sapelo Sound in the northern sector of the domain was larger than observations. Indeed, salinity variability at the head of Sapelo Island is correlated with local precipitation (Fig. 3), suggesting that simply neglecting freshwater input in that region could result in salinity bias. To address this disparity, a small freshwater discharge was introduced at the head of Sapelo Sound, using the same temporal variability observed at the Altamaha River. Sensitivity experiments were pursued, and it was determined that imposing a freshwater input equivalent to 5% of the discharge at the Altamaha River minimized the bias between modeled and observed salinity at Sapelo Sound. The input of freshwater at Sapelo River at the head of Sapelo Sound acted as a crude attempt to capture the known input of an unknown quantity of freshwater by groundwater inflow and surface runoff associated with local precipitation (Fig. 3).

Model analyses presented here are focused on 2008, a year when the seasonal evolution of river discharge was similar to the long-term average. Observations collected at multiple moorings as part of the Georgia Coastal Ecosystem Long Term Ecological Research (GCE-LTER) project (Di Iorio and Castelao 2013; see Fig. 4 for location of stations) were used for model evaluation. Precipitation data was also collected as part of the GCE-LTER project.

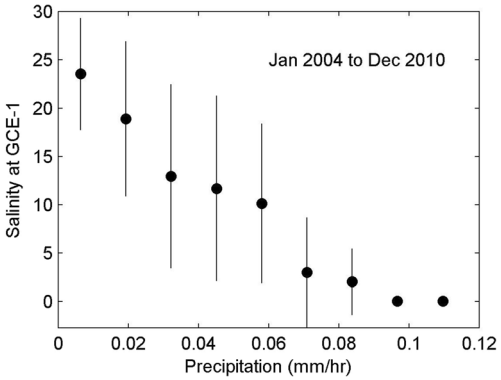

Fig. 3 Binned scatterplot of precipitation (measured near GCE-6) and salinity near the head of Sapelo Sound (GCE-1) for January 2004 to December 2010. See Fig. 4 for location of stations. Precipitation data was convoluted with a one-sided, exponentially decaying filter (Austin and Barth 2002) with a decay scale of 26 days

In order to investigate water movement within the estuary and between the estuary and the coastal ocean, FVCOM's three-dimensional Lagrangian particle tracking module was used. A total of 5643 particles were initially distributed over the main channels and tidal creeks. Particle density distribution was higher in regions where the grid spacing was smaller (i.e., in tidal creeks, especially near uplands). No particle was released over the shelf (see Fig. 5c for delineation of the area where particles were released). Particles were released near the bottom and tracked for 60 days in early March, early

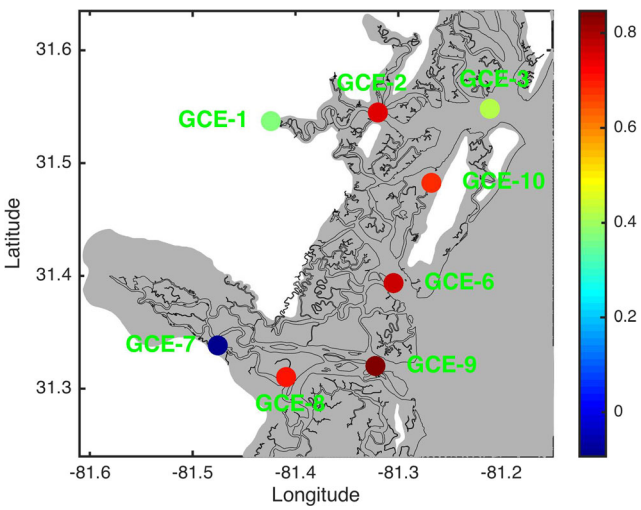

Fig. 4 Location of GCE-LTER stations where time series of salinity are available. *Colors* indicate correlation coefficients between modeled and observed salinity. *Black* contour shows mean sea level

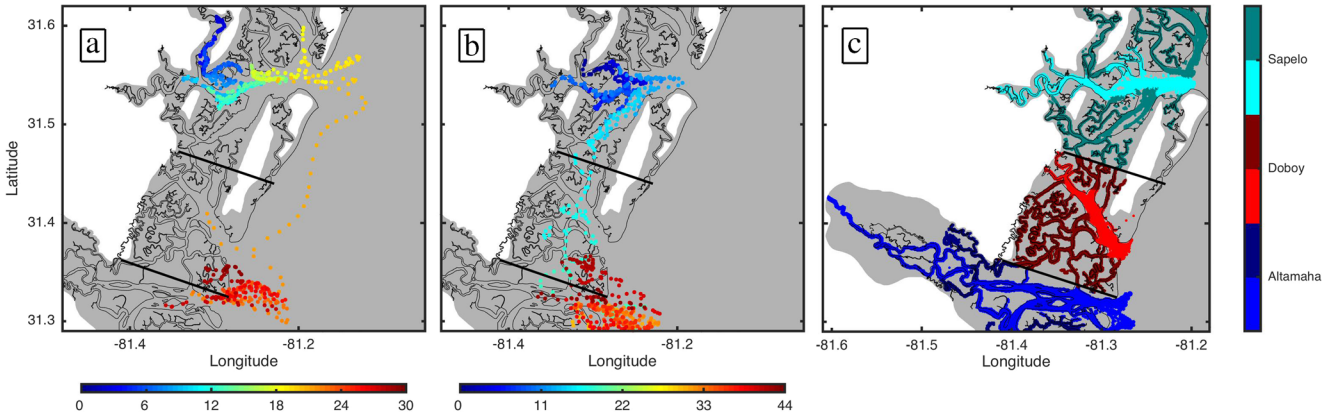

Fig. 5 Example of the trajectories of two particle (*dots*) released at Sapelo Sound in mid-August that were connected to the other subdomains via the **a** coastal or **b** estuarine pathways. *Colors* represent time since particle release in days. Time interval between successive positions is 1 h. **c** Delineation of the different subdomains: Altamaha River (*blue*), Doboy Sound (*red*), and Sapelo Sound (*cyan*). Main channels are indicated by *lighter colors*. *Black thick lines* in all panels show boundaries of the subdomains. No particle was released in the area shown in *gray* on panel (**c**). In all panels, *black* contour shows mean sea level

June, mid-August, and mid-November (green lines on Fig. 2) to capture the influence of seasonal variations in river discharge and wind forcing (even though particles were released near the bottom, they could be observed throughout the water column soon after their release). The early-March release captured the peak in river discharge. Early June and mid-August represented periods of low river discharge at the beginning and near the end of the period of dominant upwelling-favorable winds, respectively. At mid-November, river discharge was low and winds were predominantly downwelling favorable. In each case, particles were released six times regularly spaced temporally throughout a single tidal cycle between consecutive troughs. During the simulations, about 15% of the particles became artificially trapped in the salt marsh and stopped moving indefinitely. Those particles were discarded from all subsequent analyses.

The Lagrangian particle tracking scheme was used to quantify timescales, connectivity, and transport pathways in the system. The local residence time (Dronkers and Zimmerman 1982) at each node in the finite volume mesh was determined by the average time it took for the 100 particles that were released closest to a particular node to exit the estuary, weighted by the inverse of the distance (e-folding scale of 1000 m) between the node and the initial position of the particle. That computation is repeated six times for each node, once for each particle release uniformly distributed temporally throughout a tidal cycle. The tidally averaged local residence time (referred to simply as local residence time) was computed as the average of these six estimates. The standard deviation of these six estimates (i.e., the six tidal phase dependent estimates) was also computed to obtain a measure of variability in local residence time as a function of the phase of the tide at the time of the particle release. We note that particles are often transported back into the estuary by tidal currents after leaving the estuary for the first time. Here, the local residence time was computed based on the timing when the particle left the estuary for the first time.

Particle trajectories were also used to identify connectivity between the different channels, tidal creeks, and intertidal areas. For that, the entire estuary was once again divided into three subdomains representing the Altamaha River and Doboy and Sapelo Sounds. The trajectory of each particle was then used to determine which subdomains (Fig. 5c) were visited by the respective particle. In the example shown in Fig. 5a, a particle was released near the head of Sapelo Sound. The particle was first transported offshore into the coastal ocean, and subsequently into Doboy Sound and then into the Altamaha River. In the example shown in Fig. 5b, another particle released at Sapelo Sound was also transported into Doboy Sound and the Altamaha River. In that case, however, the particle was transported through the network of creeks and channels connecting the different subdomains. In both those cases, the particles were considered to have visited all three subdomains. Connectivity was defined for each node as the subdomains visited by the particle closest to the respective node. We note that a given node was considered connected to a given estuary even if a particle reached that estuary in only one of the six simulations where particles were released at different phases of the tidal cycle. In other words, if a particle closest to a given node reached a subdomain in any of the six releases, then that node was considered connected to that subdomain. That calculation was repeated for the particle release experiments during the four seasons, allowing for identification of how connectivity in the estuary varied as a function of river discharge and wind forcing.

Lastly, we also identified the pathways by which the node was connected to a given subdomain. In the example shown in Fig. 5a, the particle was first transported out into the coastal

ocean, and then back into Doboy Sound and the Altamaha River. We refer to this as the coastal pathway. In other instances, however, as shown in Fig. 5b, particles move between the subdomains via the network of channels and tidal creeks, in which case the node was considered connected to the subdomains via the estuarine pathway. Since there were six particle releases for each season (i.e., at different phases of the tidal cycle), each node can be connected to a given subdomain by both the coastal and the estuarine pathways.

Model Evaluation and Salinity Variability in the System

Model results were compared with time series of salinity from eight moorings deployed as part of the GCE-LTER program (Di Iorio and Castelao 2013). Correlation coefficients between modeled and observed salinity are shown in Fig. 4. Correlations varied between 0.7 and 0.85 at five out of the eight stations, and were statistically significant at the 95% confidence level. At GCE-7, correlation was weak and not statistically significant. That station is located substantially upstream along the Altamaha River, and it is characterized by near zero salinity most of the time. As such, salinity variability is often dominated by noise or by weak events that were not well represented in the model. Correlations were also relatively weak (although still significant) at GCE-1 and GCE-3. A decrease in correlation coefficients between the Altamaha River (GCE-8 and GCE-9) and Sapelo Sound was expected. This is because salinity variability at the Altamaha is strongly forced by river discharge (Alber and Sheldon 1999b), which is considered in the model. Salinity variability at the head of Sapelo Sound at GCE-1, on the other hand, is strongly influenced by local runoff and/or groundwater inputs recharged by precipitation (Fig. 3), which were not directly considered in this study. The correlation coefficient is also reduced near the mouth of Sapelo Sound at station GCE-3 (Fig. 4). That drop in correlation may be related to the somewhat idealized nature of the simulation since time variations in offshore hydrography along the boundaries were not considered. It is possible, for example, that at least some of the variability in salinity in that region is related to freshwater input farther north beyond the boundary of the domain (e.g., Ogeechee and Savannah rivers) that is then transported southward in a buoyancy-driven coastal current (Blanton and Atkinson 1983).

Additional model evaluation was pursued by comparing the correlation and lags between river discharge and salinity in the model and in the observations. Using in situ data from the GCE-LTER moorings (see Fig. 4 for location), Di Iorio and Castelao (2013) showed that correlations between discharge and salinity show average time lags ranging from 4 days in the Altamaha estuary to 12 days in Sapelo Sound. Model results were consistent with the observations, with maximum correlation between river discharge and salinity occurring for lags of 4–6 days at the Altamaha estuary and for lags of 10–16 days at Sapelo Sound (Fig. 6). This suggests that the model was able to capture not only salinity variability in the system, but also the dynamic response to changes in river discharge, including the lag in the response observed between the Altamaha estuary and Sapelo Sound farther north. It is interesting to note that at the upstream sector of the Altamaha River, salinity was not significantly correlated to river discharge. Those locations are almost always fresh except for times of drought conditions (Di Iorio and Castelao 2013). As such, increases in river discharge often do not result in decreases in salinity (since the water is already fresh most of the time), resulting in low correlation in that region. Another area of low correlation is near the mouth of Sapelo Sound. Analysis of mooring observations reveal that the region is characterized by significant correlation between river discharge and salinity (Di Iorio and Castelao 2013), indicating that the model was not able to properly capture the dependence of salinity variability to river discharge in that part of the domain. This is consistent with the low correlations between modeled and observed salinity reported earlier for GCE-3 (Fig. 4).

Maps of mean salinity and standard deviation in the estuary are shown in Fig. 7. River inflow in the South Atlantic Bight is

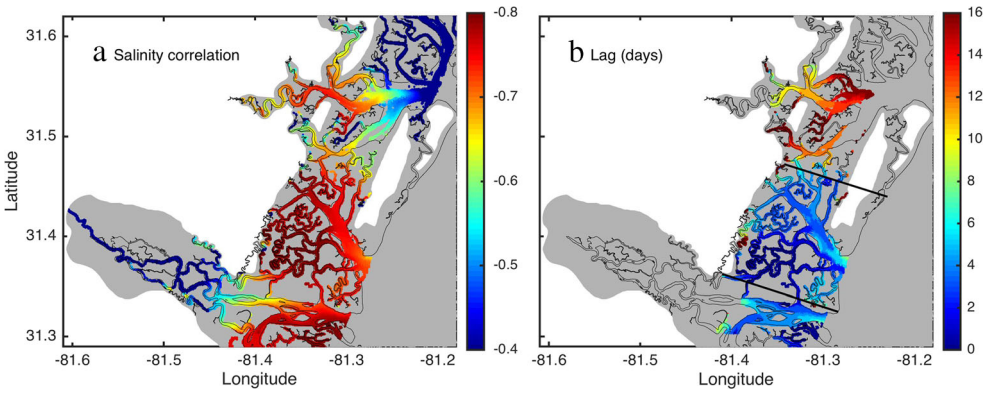

Fig. 6 **a** Correlation coefficient and **b** time lag (in days) between river discharge and salinity over the estuary. Time lags at locations where the correlation is not statistically significant are not shown. *Black* contour shows mean sea level. *Black thick lines* in (**b**) show boundaries of the subdomains (Altamaha River, Doboy Sound, and Sapelo Sound)

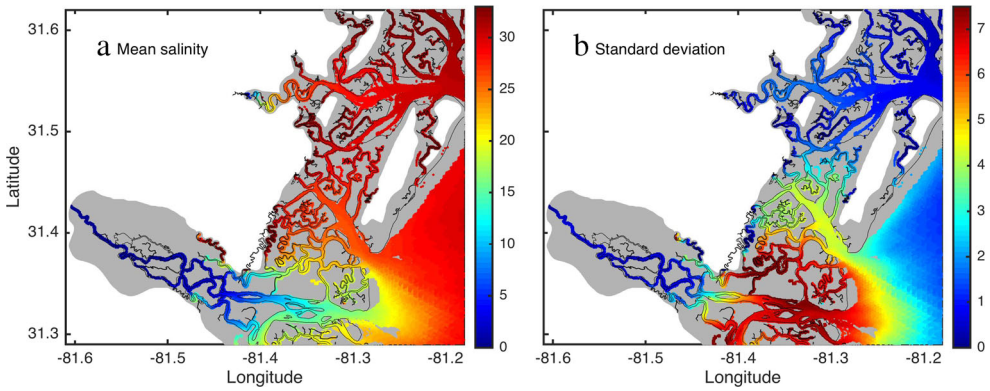

Fig. 7 **a** Average and **b** standard deviation of salinity over the domain. *Black* contour shows mean sea level

a major driver of salinity variability on the inner shelf (Blanton and Atkinson 1983). As expected, average salinity was low in the Altamaha River, increasing offshore and to the north toward Doboy and Sapelo Sounds. Small creeks and channels connecting the Altamaha River and Doboy Sound were also characterized by low average salinities, suggesting that some of the freshwater from the Altamaha River leaked into Doboy Sound via those channels. Low average salinity was also observed near the head of Sapelo Sound, a result also observed based on in situ data (Di Iorio and Castelao 2013). It is important to point out, however, that the correlation between observation and model results was comparatively low in that area (Fig. 4). More interestingly, the map of standard deviation of salinity in the estuary revealed the areas that were characterized by high variability. The most obvious feature is the high values observed near the mouth of the Altamaha River extending into the coastal ocean, where strong mixing between river and shelf water occurs (Di Iorio and Kang 2007). High variability was also observed in the creeks connecting the Altamaha River and Doboy Sound, once again supporting the interpretation that those channels can play an important role connecting the different subdomains (Di Iorio and Castelao 2013). An empirical orthogonal function (EOF) decomposition of the surface salinity field (not shown) revealed a spatial pattern for the dominant mode that was very similar to the standard deviation map shown in Fig. 7b. The amplitude time series of the dominant mode, which explains 84.4% of the total variance, was highly correlated with river discharge ($r = 0.84$), revealing that most of the salinity variability described above (Fig. 7b) was related to variability in river inflow.

Although Doboy and Sapelo Sounds were both characterized by high average salinity, there was a remarkable difference in salinity standard deviation between the two subdomains. Doboy Sound was characterized by high variability, revealing a large degree of influence from low-salinity water from the Altamaha River. Analysis of individual maps of salinity revealed that, in addition to low-salinity water leaking into Doboy Sound via small channels and creeks, as described above, low-salinity water also enters Doboy Sound via the mouth during flood tides. Salinity variability decreases substantially between Doboy and Sapelo Sound, so that salinity standard deviation in the northern sector of the domain, farther from the river, was substantially smaller. The sharp decrease along the channels between Doboy and Sapelo Sound may be related to nodal points that are often observed in interconnected estuaries, produced by simultaneous tidal forcing from both ends of the channel (Traynum and Styles 2008).

Local Residence Time

Maps of local residence time for each season are shown in Fig. 8. There is a general tendency, regardless of the season, for local residence times to increase with increasing distance from the ocean. Near the mouth of each sound, the local residence times approach zero since particles are easily transported offshore onto the shelf during a tidal cycle. Analyses of individual particle trajectories indicate that the excursion length of the tides near the mouth of the estuaries is of the order of 6–8 km. The largest local residence times are observed in small creeks bordering uplands near the head of the sounds. Since those areas are more likely to be developed, any input of contaminants or nutrients due to anthropogenic activities can potentially have a relatively large impact on estuarine water quality, given the comparative large local residence time observed in those areas. The increase in local residence times as a function of distance from the mouth is more easily observed when the local residence times are averaged along the main channels of each Sound (i.e., along the lighter shaded regions delineated in Fig. 5c). In all cases, local residence times increase from nearly zero close to the mouth to several days upstream (Fig. 9).

Comparison among the different subdomains revealed substantial differences in local residence time in the system (Figs. 8 and 9). Values are smallest in the Altamaha River during spring, when strong river discharge (Fig. 2) contributes to the rapid transport of the particles toward the shelf, which is consistent with Alber and Sheldon's (1999a) results. The local

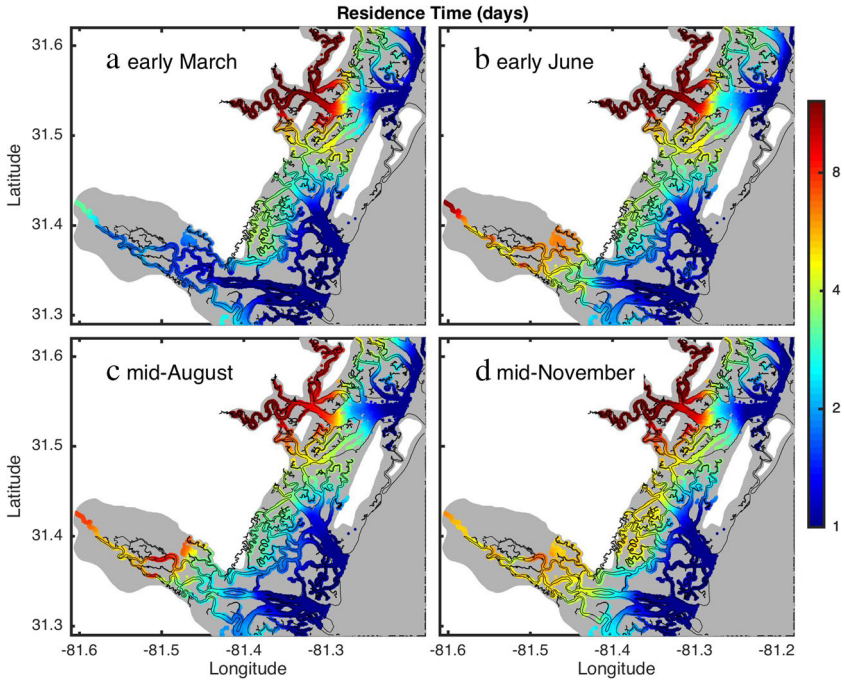

Fig. 8 Maps of local residence time (in days) for early March, early June, mid-August, and mid-November. A nonlinear color scale is used to reveal as much as possible of the spatial structure. *Black* contour shows mean sea level

residence time more than doubles in the Altamaha River in the other seasons when river discharge is reduced (Fig. 9). The transit time, defined as the total amount of time it takes for freshwater to transit through an estuary, has been previously estimated for the Altamaha River to vary between 1.6 and 9 days for river flow exceeding 100 m^3 s^{-1} (Sheldon and Alber 2005). That is comparable to our estimates of local residence time at the head of the Altamaha River, which range from about 2.5 days during high river discharge conditions to about 7 days for low river flow (Figs. 8 and 9). For a given distance from the mouth, the local residence time at Doboy Sound is generally larger than at the Altamaha River (Fig. 9; a dashed gray line with the same slope is shown in all panels for reference), likely because of reduced influence of direct river

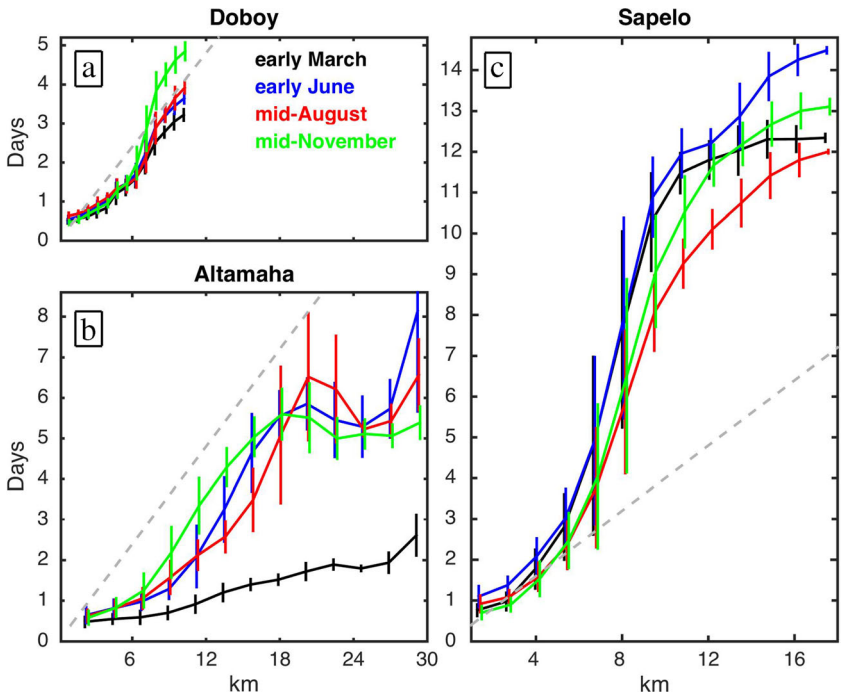

Fig. 9 Local residence time (in days) averaged along the main channels (see Fig. 5c for channel delineation) of **a** Doboy Sound, **b** Altamaha River, and **c** Sapelo Sound in different seasons as a function of distance from the mouth. A *gray dashed line* with the same slope is plotted in all panels for reference. Note that a different *x*-axis is used on panel (**c**)

discharge at Doboy Sound. The increase in local residence time compared to the Altamaha River is especially true for the complex network of channels and creeks near the uplands to the southwest of the main channel at Doboy Sound (around 81.35°–81.4°W, 31.37°–31.44°N), where the local residence time during late fall can be in excess of 5 days. At Sapelo Sound, on the other hand, the local residence time is significantly larger, especially from the mid-estuary to its head (Figs. 8 and 9). At those locations, the local residence time is large regardless of the season. A small reduction in local residence time is observed during mid-August after the region is exposed to strong and persistent upwelling-favorable winds. For any given distance from the estuary mouth, local residence time at Sapelo Sound exceeds the local residence time at the Altamaha River and Doboy Sound for all seasons (Fig. 9; compare different curves with gray line for reference).

It is interesting to note that in some seasons, a local maximum in residence time is observed around 20 km in the Altamaha River (Fig. 9). Detailed analysis of individual particle trajectories reveals that in some cases, particles released in one or more of the multiple channels in that area become trapped in recirculation regions, while particles released upstream may continue their trajectory to the ocean via another channel. That is particularly clear in the spatial distribution of local residence time during low discharge conditions (Fig. 8b–d), for example, when the local residence time is smaller in the southern channel of the river (around −81.51°W, 31.35°N) compared to the northern channels (around −81.49°W, 31.38°N).

Analysis of maps of the standard deviation of the local residence time among the six particle release experiments in each season (i.e., the six tidal-phase-dependent estimates) scaled by the respective tidally averaged local residence times (Fig. 10) reveals that variability as a function of the phase of the tidal cycle is small, except near the mouths of the estuaries. At those regions near the ocean, while a particle released at ebb tides can be quickly exported, a particle released at low tides will be first transported into the estuary by flood currents and only subsequently exported. Since the local residence time is small in that area, the relative measure of variability shown in Fig. 10 is large, reaching 80% in some locations. Away from the mouth of each sound, however, the standard deviation is small compared to the average of the six simulations, indicating that the patterns described before (Fig. 8) are robust and not strongly dependent on the phase of the tidal cycle in which particles were released.

Connectivity and Transport Pathways

Results shown in the previous section have revealed large spatial and temporal variations in local residence time in the estuarine system. Here, the connectivity and transport pathways between the subdomains were investigated to identify how particles move within the system. Specifically, we tracked the trajectory of each particle released in the model and identified which parts of the estuary the particle was transported to (Fig. 11). The release location of a particle that was found at the Altamaha River and at Doboy Sound at some point in its trajectory, but not at Sapelo Sound, is marked in green in Fig. 11, for example. If a particle was found at the Altamaha River and at Doboy and Sapelo Sounds at some point in its trajectory, on the other hand, then its release location is marked in yellow, and so on.

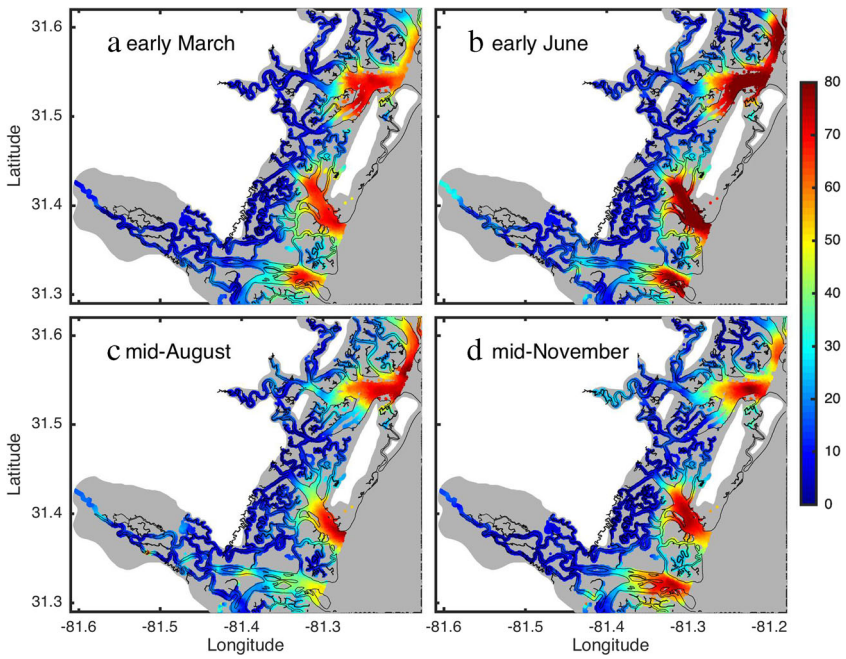

Fig. 10 Maps of the ratio between the standard deviation of the local residence time among the six particle release experiments at different phases of the tidal cycle and the respective tidally averaged local residence time in each season. Values have been multiplied by 100 to yield a percentage. *Black* contour shows mean sea level

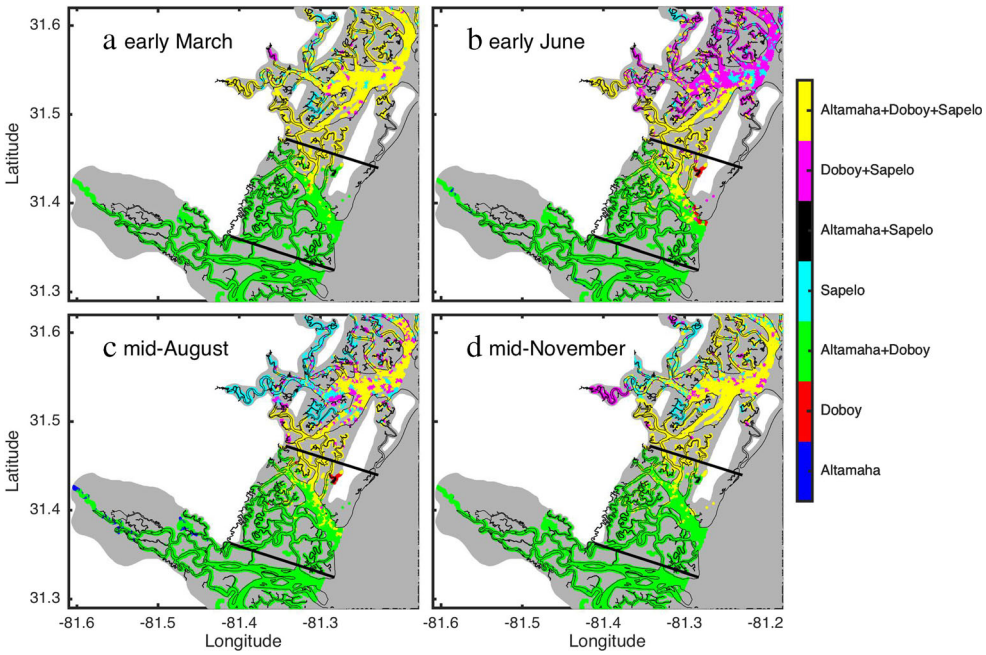

Fig. 11 Maps of connectivity in each season. *Black* contour shows mean sea level. *Black thick lines* in all panels show boundaries of the subdomains (Altamaha River, Doboy Sound, and Sapelo Sound)

There is a generally tendency for the Altamaha estuary and Doboy Sound to be connected to each other regardless of the season. It is interesting to note that there is a divide in connectivity approximately along the center of the main channel in Doboy Sound. While particles released in the southern part of the channel are restricted to Doboy Sound and the Altamaha River (shown in green), particles released in the northern part of the channel generally also reach Sapelo Sound (shown in yellow), especially during early June and mid-August (Fig. 11).

The fact that most particles released in the Altamaha River and in (at least the southern half of) Doboy Sound are not transported into Sapelo Sound can help explain the large difference in salinity standard deviation between those subdomains (Fig. 7b). The connectivity between Doboy Sound and the Altamaha River indicates that low-salinity water from the river is easily transported into Doboy Sound (Fig. 11). This is consistent with the numerical simulations of Di Iorio and Castelao (2013), which revealed that a large amount of freshwater introduced in the Altamaha River could be transported into their idealized representation of Doboy Sound. Once at Doboy Sound, however, the low-salinity water is not easily transported into Sapelo Sound (Figs. 11). This limited connectivity would result in reduced salinity variability and increased mean values in the northern part of the domain, consistent with the model results (Fig. 7).

Creeks and channels between Doboy and Sapelo Sounds are remarkable in the sense that they are regions connected to all estuaries year-round. Specifically, particles released in that region are able to reach all subdomains in all seasons (shown in yellow in Fig. 11). The downstream sector of the main channel of Sapelo Sound is also connected to the other estuaries year-round. Therefore, although most particles released at the Altamaha River or Doboy Sound are not transported into Sapelo Sound, a large fraction of the particles released at the downstream half of Sapelo Sound are transported into Doboy Sound and into the Altamaha River (shown in yellow in Fig. 11; the exception is the early June release, when most particles—shown in purple—do not reach the Altamaha River). A different pattern is observed upstream near the head of Sapelo Sound in mid-August and mid-November, however. During that time, many particles are either constrained to Sapelo Sound itself or they may reach Doboy Sound in a few cases, but not the Altamaha River (Fig. 11).

Further information about water exchange can be obtained by investigating transport pathways in the system (Fig. 12). The connectivity maps demonstrated that particles released at the Altamaha River can reach Doboy Sound, and vice versa, in all seasons (Fig. 11). Analysis of the transport pathways reveals that particles released at the River can reach Doboy Sound by both the coastal and the estuarine pathways most of the time (Fig. 12). The only exception is during the peak in river discharge (early March, Fig. 12a, e), when careful examination reveals that particles released in the southern part of the Altamaha River near the mouth only reach Doboy Sound via the coastal pathway. Particles released in several of the creeks between the Altamaha River and Doboy Sound only reach both subdomains via the estuarine pathway, with the exception of high river discharge conditions during spring, when both pathways are available. This demonstrates that the network of creeks between the main channels of the Altamaha River and Doboy Sound plays an important role connecting those two systems. The analysis also indicates that

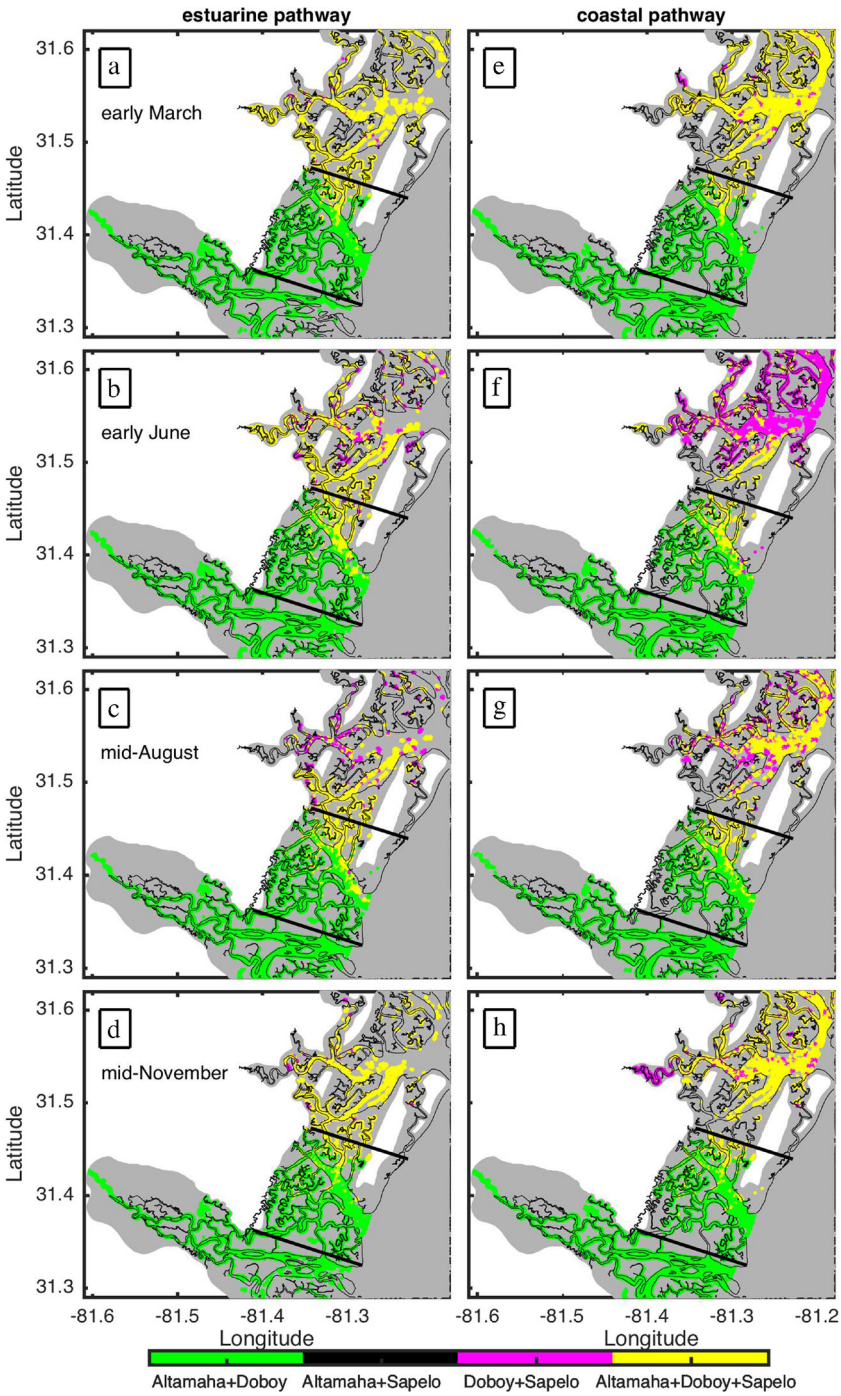

Fig. 12 Maps of transport pathways in the system. Estuarine pathway is shown on the *left*, while coastal pathway for each season is shown on the *right*. *Black* contour shows mean sea level. *Black thick lines* in all panels show boundaries of the subdomains (Altamaha River, Doboy Sound, and Sapelo Sound)

most particles released at the downstream sector of Sapelo Sound reach the Altamaha River and Doboy Sound via the coastal pathway (Fig. 12e–h). Transport through the estuarine pathway is much more restricted (Fig. 12a–d).

The analysis presented here provides an unprecedented view of connectivity and transport pathways in the estuarine system, revealing substantial spatial and temporal variability. This variability can have large implications for the ecosystem. For example, while nutrient inputs (or the input of any other material) at the Altamaha River are likely to have a large influence on the river itself and on Doboy Sound, the influence on Sapelo Sound is likely to be substantially smaller. Constituents introduced into the system with groundwater input at the network of creeks connecting Doboy and Sapelo Sound, on the other hand, are likely to influence all three subdomains. The same is true for anthropogenic inputs. Depending on the location of the input, a contaminant may be restricted to a few areas or it may be spread to all

subdomains. The large spatial variability in local residence time also indicates that, depending on the location of the input of a contaminant, it may be rapidly exported to the coastal ocean or it may remain much longer within the estuary.

Conclusions

A high-resolution coastal ocean model was used to investigate circulation and variability in adjacent estuaries off the southeastern U.S. The region is characterized by complex topography, and adjacent estuaries are interconnected by a network of channels, tidal creeks, and intertidal marshes. Comparisons with observations reveal that the model is able to capture salinity variability over most of the domain, especially along the Altamaha River and Doboy Sound, where salinity is highly correlated with river discharge with relatively short time lags. The model-data comparisons worsen near the head of Sapelo Sound, where seasonal variability in salinity is also strongly influenced by local precipitation.

Model results reveal for the first time the region characterized by high salinity variability in the system in high resolution, which extends from the downstream half of the Altamaha River to Doboy sound. The network of creeks and channels connecting the River and the Sound plays a large role on the spread of the low-salinity water in the system. Salinity variability at Sapelo Sound is substantially smaller. This is consistent with the identified preferred transport pathways in the system, which indicate that particles released at the Altamaha River or Doboy Sound do not often make it into Sapelo Sound farther north. The Altamaha estuary and Doboy Sound are connected during all seasons, with exchange occurring both via the coastal and the estuarine pathways. The local residence time is strongly variable spatially, being significantly larger at Sapelo Sound than farther south. At the Altamaha River and Doboy Sound, the local residence time is smaller during high discharge conditions, demonstrating the large influence of the river on transport processes and estuary-shelf exchange.

Acknowledgements We thank two anonymous reviewers for their thoughtful and constructive suggestions. We gratefully acknowledge support by the National Science Foundation through grant OCE 1632090 and the Georgia Coastal Ecosystems Long Term Ecological Research program (GCE-LTER, OCE-1237140). Additional support was provided by an Institutional Grant (NA100AR4170098) to the Georgia Sea Grant College Program from the National Sea Grant Office, National Oceanic and Atmospheric Administration (NOAA), U.S. Department of Commerce and by grant award NA11NOS4190113 to the Georgia Department of Natural Resources (DNR) from the Office of Ocean and Coastal Resource Management (OCRM), NOAA. All views, opinions, statements, findings, conclusions, and recommendations are those of the authors and do not necessarily reflect the opinions of NSF, the Georgia Sea Grant college Program, DNR, OCRM, or NOAA.

References

Aikman, F.A., and L.W.J. Lanerolle. 2004. Report on the National Ocean Service Workshop on Residence/Flushing Times in Bays and Estuaries. NOAA Office of Coast Survey, Silver Spring, MD. http://www.nauticalcharts.noaa.gov/csdl/residencetime.html.

Alber, M., and J.E. Sheldon. 1999a. Use of a data-specific method to examine variability in the flushing times of Georgia estuaries. *Estuarine, Coastal and Shelf Science* 49: 469–482.

Alber, M., and J.E. Sheldon. 1999b. Trends in salinities and flushing times of Georgia estuaries. In *Proceedings of the 1999 Georgia Water Resources Conference*, ed. K.J. Hatcher, 528–531. Athens: University of Georgia.

Alpine, A.E., and J.E. Cloern. 1992. Trophic interactions and direct physical effects control phytoplankton biomass and production in an estuary. Limnol. Oceanography 37. doi: 10.4319/lo.1992.37.5.0946.

Atkinson, L., T. Lee, J. Blanton, and W. Chandler. 1983. Climatology of the southeastern United States continental shelf waters. *Journal of Geophysical Research* 88: 4705–4718.

Austin, J.A., and J.A. Barth. 2002. Variation in the position of the upwelling front on the Oregon shelf. *Journal of Geophysical Research* 107(C11): 3180. doi:10.1029/2001JC000858.

Blanton, J.O., and L.P. Atkinson. 1983. Transport and fate of river discharge on the continental shelf of the southeastern United States. *Journal of Geophysical Research* 88: 4730–4738.

Blanton, B.O., A. Aretxabaleta, F.E. Werner, and H.E. Seim. 2003. Monthly climatology of the continental shelf waters of the South Atlantic Bight. *J. Geophys. Res., Oceans (1978–2012)* 108(C8): 3264.

Bumpus, D. 1973. A description of the circulation on the continental shelf of the east coast of the United States. *Progress in Oceanography* 6: 111–157.

Chen, C., G. Cowles, and R.C. Beardsley. 2006a. *An unstructured grid, finite-volume coastal ocean model: FVCOM user manual, 2nd ed., SMAST/UMASSD Tech. Rep. 06-0602*, 315. New Bedford, MA: School for Marine Science and Technology, University of Massachusetts-Dartmouth.

Chen, C., R.C. Beardsley, and G. Cowles. 2006b. An unstructured grid, finite-volume coastal ocean model (FVCOM) system: Special Issue entitled "Advances in Computational Oceanography". *Oceanography* 19(1): 78–89.

Chen, C., H. Huang, R.C. Beardsley, H. Liu, Q. Xu, and G. Cowles. 2007. A finite-volume numerical approach for coastal ocean circulation studies: comparisons with finite-difference models. *Journal of Geophysical Research* 112: C03018. doi:10.1029/2006JC003485.

Chen, C., J. Qi, C. Li, R.C. Beardsley, H. Lin, R. Walker, and K. Gates. 2008. Complexity of the flooding/drying process in an estuarine tidal-creek salt-marsh system: an application of FVCOM. *Journal of Geophysical Research* 113: C07052.

Church, T.M. 1986. Biogeochemical factors influencing the residence time of microconstituents in a large tidal estuary, Delaware Bay. *Marine Chemistry* 18: 393–406.

De Brauwere, A., B. de Brye, S. Blaise, and E. Deleersnijder. 2011. Residence time, exposure time and connectivity in the Scheldt Estuary. *J. Mar. Sys.* 84: 85–95. doi:10.1016/j.jmarsys.2010.10.001.

Di Iorio, D., and R.M. Castelao. 2013. The dynamical response of salinity to freshwater discharge and wind forcing in adjacent estuaries on the Georgia coast. *Oceanography* 26(3): 44–51. doi:10.5670/oceanog.2013.44.

Di Iorio, D., and K.R. Kang. 2007. Variations of turbulent flow with river discharge in the Altamaha River Estuary, Georgia. *Journal of Geophysical Research* 112: C05016.

Dronkers, J., and J.T.F. Zimmerman. 1982. *Some principles of mixing in tidal lagoons. Oceanologica Acta*, 107–117. Bordeaux, France:

Proceedings of the International Symposium on Coastal Lagoons 9–14 September, 1981.

Duarte, A.A.L.S., and J.M.P. Vieira. 2009. Effect of tidal regime on estuarine residence time spatial variation. In *Energy, environment, ecosystems, development and landscape architecture*, ed. N. Mastorakis, C. Helmis, C.D. Papageorgiou, C.A. Bulucea, and T. Panagopoulos, 240–245. WSEAS Press.

Egbert, G.D., and S.Y. Erofeeva. 2002. Efficient inverse modeling of barotropic ocean tides. *Journal of Atmospheric and Oceanic Technology* 19: 183–204. doi:10.1175/1520-0426(2002)019<0183:EIMOBO>2.0.CO;2.

Fanning, J. L. (2003), Water use in Georgia, 2000; and trends, 1950–2000. Proceedings of 2003 Georgia Water Resources Conference, Univ. of Georgia, Athens.

Geyer, W.R. 1997. Influence of wind on dynamics and flushing of shallow estuaries. *Estuarine, Coastal and Shelf Science* 44: 713–722.

Geyer, W.R., and R. Signell. 1992. A reassessment of the role of tidal dispersion in estuaries and bays. *Estuaries* 15: 97–108. doi:10.2307/1352684.

Lee, T.N., and D.A. Brooks. 1979. Initial observations of current, temperature and coastal sea level response to atmospheric and Gulf Stream forcing on the Georgia shelf. *Geophysical Research Letters* 6: 321–324.

Lemagie, E.P., and J.A. Lerczak. 2015. A comparison of bulk estuarine turnover timescales to particle tracking timescales using a model of the Yaquina Bay Estuary. *Estuaries and Coasts* 38: 1797–1814. doi:10.1007/s12237-014-9915-1.

Medeiros, P.M., M. Seidel, T. Dittmar, W.B. Whitman, and M.A. Moran. 2015. Drought-induced variability in dissolved organic matter compostion in a marsh-dominated estuary. *Geophysical Research Letters* 42(15): 6446–6453.

Mellor, G.L., and T. Yamada. 1982. Development of a turbulent closure model for geophysical fluid problems. *Reviews of Geophysics* 20: 851–875.

Menzel, D.W. 1993. Ocean processes: U.S. southeast continental shelf. A summary of research conducted in the South Atlantic Bight under the Auspices of the U.S. Department of Energy from 1977 to 1991, Publ. DOE/OSTl-11674, 112, Off. of Sci. and Tech. Inf., U.S. Dep. of Energy, Washington, D. C.

Monsen, N., J.E. Cloern, and L.V. Lucas. 2002. A comment on the use of flushing time, residence time, and age as transport time scales. *Limnology and Oceanography* 47: 1545–1553.

Moore, W.S. 1996. Large groundwater inputs to coastal waters revealed by ^{226}Ra enrichments. *Nature* 380.

Moore, W.S. 2010. The effect of submarine groundwater discharge on the ocean. *Annual Review of Marine Science* 2: 59–88.

Pietrafesa, L.J., J.O. Blanton, J.D. Wang, V.H. Kourafalou, T.N. Lee, and K.A. Bush. 1985. The tidal regime in the South Atlantic Bights. In *Oceanography of the southeastern U.S. continental shelf*, ed. L.P. Atkinson, D.W. Menzel, and K.A. Bush, 63–76. Washington, D. C: AGU.

Ralston, D.K., W.R. Geyer, and J.A. Lerczak. 2010. Structure, variability, and salt flux in a strongly forced salt wedge estuary. *Journal of Geophysical Research* 115: C06005. doi:10.1029/2009JC005806.

Rasmussen, B., and A. Josefson. 2002. Consistent estimates for the residence times of micro-tidal estuaries. *Estuarine, Coastal and Shelf Science* 54: 65–73.

Sheldon, J.E., and M. Alber. 2002. A comparison of residence time calculations using simple compartment models of the Altamaha River estuary, Georgia. *Estuaries and Coasts* 25: 1304–1317. doi:10.1007/bf02692226.

Sheldon, J.E., and M. Alber. 2005. Comparing transport times through salinity zones in the Ogeechee and Altamaha river estuaries using squeezebox. In *Proc 2005 Georgia Water Res Conf*, ed. K.J. Hatcher. Athens: The University of Georgia.

Sheldon, J.E., and A.B. Burd. 2014. Alternating effects of climate drivers on Altamaha River discharge to coastal Georgia, USA. *Estuaries and Coasts* 37: 772–788.

Tebeau, P.A., and T.N. Lee. 1979. *Wind induced circulation on the Georgia shelf, (winter 1976/77) RSMAS Tech Rep. 79003*. Miami, Fla: Univ. of Miami.

Traynum, S., and R. Styles. 2008. Exchange flow between two estuaries connected by a shallow tidal channel. *J. Coastal Res.* 24(5): 1260–1268. doi:10.2112/07-0840r.1.

Weber, A.H., and J.O. Blanton. 1980. Monthly mean wind fields for the South Atlantic Bight. *Journal of Physical Oceanography* 10(8): 1256–1263. doi:10.1175/1520-0485(1980)010<1256:MMWFFT>2.0.CO;2.

Zhao, L., C. Chen, J. Vallino, C. Hopkinson, R.C. Beardsley, H. Lin, and J. Lerczak. 2010. Wetland-estuarine-shelf interactions in the Plum Island Sound and Merrimack River in the Massachusetts coast. *Journal of Geophysical Research* 115: C10039. doi:10.1029/2009JC006085.